

## Design of a dinuclear ruthenium based catalyst with a rigid xanthene bridge for catalytic water oxidation



Zhao Liu, Yan Gao\*, Min Zhang, Jianhui Liu

State Key Laboratory of Fine Chemicals, Institute of Artificial Photosynthesis, DUT-KTH Joint Education and Research Center on Molecular Devices, Dalian University of Technology (DUT), Dalian 116024, PR China

### ARTICLE INFO

#### Article history:

Received 5 February 2015

Received in revised form 5 March 2015

Accepted 9 March 2015

Available online 12 March 2015

#### Keywords:

Ruthenium dimer catalyst

Water oxidation

Mechanism

Kinetic study

### ABSTRACT

A new dinuclear ruthenium complex **1** ( $\text{L1}[\text{Ru}(\text{bda})_2(\text{picoline})]_2$ ) based on Ru–bda ( $\text{H}_2\text{bda} = 2,2'$ -bipyridine-6,6'-dicarboxylic acid) and dipyriddy xanthene (**L1** = 4,5-dipyridyl-2,7-di-tert-butyl-9,9-dimethyl xanthene) ligand was synthesized to probe the catalytic oxidation of water. An oxygen evolution experiment displays a low catalytic water oxidation activity with a first-order reaction kinetic mechanism. The result indicates that the O–O bond formation of the dinuclear catalyst **1** follows a water nucleophilic attack pathway rather than a radical coupling pathway. The most plausible interpretation is that the steric hindrance effects of the **L1** and bda ligands lead to a disadvantage in forming the face-to-face configuration of the two active sites in a one dimer molecule.

© 2015 Elsevier B.V. All rights reserved.

Splitting water into oxygen and hydrogen is a great potential approach to develop an alternative renewable energy source to overcome the looming shortfall in fossil fuels [1–7]. The key challenge in water splitting is the development of highly active and robust catalysts for water oxidation [8–10]. Hence, with the gradual understanding of the water oxidation complex in photosystem II, many models based on transition metals have been developed aimed at this objective. Consequently several manganese, ruthenium, and cobalt complexes have been reported for water oxidation [11–13]. In principle, developing molecular catalysts is regarded as the most potential and prospective way to achieve highly efficient catalytic water oxidation, especially for developing mono- or multinuclear metal based molecular catalysts with relatively large turnover numbers (TONs). In these studies, much attention about dinuclear molecular catalysts has been paid [14] to mimic the functional  $\text{Mn}_4\text{Ca}$  cluster in the oxygen evolution center (OEC), such as the famous “blue dimer” [15], and some dinuclear mutipyridyl dicarboxyl ruthenium complexes [16,17].

Recently, a series of mononuclear ruthenium catalysts  $[\text{Ru}(\text{bda})\text{L}_2]$  ( $\text{H}_2\text{bda} = 2,2'$ -bipyridine-6,6'-dicarboxylic acid, L = N-donor ligands) have been developed with high TON and turnover frequency (TOF) [18]. More interestingly, research shows that a  $[\text{Ru}(\text{bda})\text{L}_2]$  catalyst undergoes a radical coupling pathway between two  $\text{Ru}^{\text{V}}=\text{O}$  intermediates, and a very uncommon seven-coordinate Ru (IV) dimeric ruthenium intermediate **M** (Fig. 1) was successfully isolated [19].

As known, xanthene is usually used as a bridge to connect the dual catalytic centers. The acid–base functionality is positioned from a

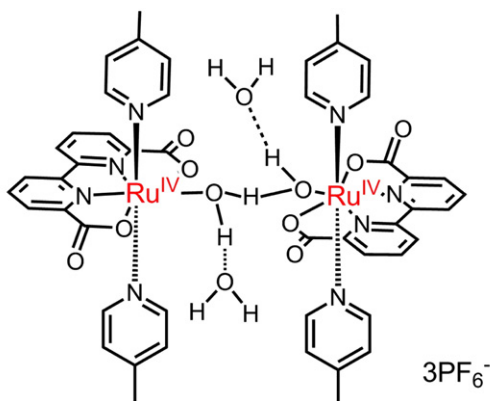
xanthene spacer over the face of a redox-active macrocycle [20]. Therefore, it was motivated by those successful xanthene dinuclear complexes and the  $\text{Ru}(\text{bda})\text{L}_2$  type of catalysts. A new dinuclear complex  $\text{L1}[\text{Ru}(\text{bda})_2(\text{picoline})]_2$  (**L1** = 4,5-dipyridyl-2,7-di-tert-butyl-9,9-dimethyl xanthene) was designed and synthesized to approach highly catalytic water oxidation. Hence, we report the spectroscopic and electrochemical characterization of the new Ru dinuclear WOC, together with an ordinary mechanistic description of the water oxidation reaction supported by kinetic study.

The synthesis of the new dinuclear Ru catalyst was reported (Scheme 1). It is obtained in a one step co-ordination reaction between xanthene **L1** and  $\text{Ru}(\text{bda})(\text{DMSO})_2$  **M1** with a mole ratio of 2:1. The mixture is refluxed for 16 h to give the desired dinuclear Ru–bda complex **1** with a yield of 35%.

Complex **1** displayed a relatively stable chemical property at room temperature, and its spectroscopic characterizations by  $^1\text{H}$  NMR, high resolution mass spectrometry (HRMS), and UV–vis were performed to verify the structural properties. The  $^1\text{H}$  NMR spectrum of complex **1** displayed two big singlet peaks at  $\delta = 1.38$  and 1.70 ppm that were assigned respectively to the proton resonances of C–H in the tertiary butyl and methanyl groups of xanthene ligand. Another big singlet peak at  $\delta = 2.23$  ppm was assigned to the proton resonance of C–H in the methanyl group of axial pyridine ligands. Moreover, the typical doublet peak at  $\delta = 8.92$  ppm was assigned to protons on the equatorial ligand of the bda ligand. The result confirmed the structure of complex **1** and indicated that the xanthene ligand has been successfully introduced. In addition, high resolution mass spectrometry (HRMS) was also used to characterize this compound with a micromass Q-TOF Micro by TOF MS ESI+ (positive mode). The HRMS spectrum of

\* Corresponding author.

E-mail address: [dr.gaoyan@dut.edu.cn](mailto:dr.gaoyan@dut.edu.cn) (Y. Gao).



$$\mu\text{-(HOHOH)-[Ru}^{\text{IV}}(\text{bda})(\text{picoline})_2\text{]}_2(\text{PF}_6)_3\text{-(H}_2\text{O)}_2 \text{ M}$$

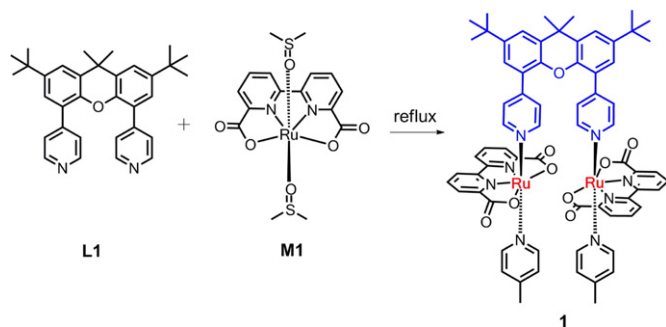
Fig. 1. Structure of ruthenium dimer **1**.

complex **1** ( $\text{M} = \text{C}_{69}\text{H}_{62}\text{N}_8\text{O}_9\text{Ru}_2$ ) showed two signals at 1350.2725 and 1351.2802 that were assigned respectively to the species of  $[\text{M}]^+$  and  $[\text{M} + \text{H}]^+$ , which were fit very well to the calculated data of 1350.2727  $[\text{M}]^+$  and 1351.2805  $[\text{M} + \text{H}]^+$ .

The UV–vis spectrum of catalyst **1** in  $\text{CH}_2\text{Cl}_2$  was measured (Fig. 2). The two types of absorption bands at  $\lambda_{\text{max}} = 250$  and 305 nm are assigned to the absorption of  $\text{bda}-\pi \rightarrow \text{bda}-\pi^*$  electron transition. The strong absorption band of complex **1** at  $\lambda_{\text{max}} = 395$  nm is reasonably assigned to the MLCT band of  $\text{Ru}-d \rightarrow \text{bda}-\pi^*$ , since a bda ligand bearing two carbonyl units has a lower  $\pi^*$  orbital.

The cyclic voltammogram (CV) of complex **1** was recorded in anhydrous  $\text{CH}_2\text{Cl}_2$  with a 0.1 M electrolyte ( $\text{NH}_4\text{PF}_6$ ) (Fig. 3a). The dinuclear catalyst **1** shows three reversible redox peaks; the first two reversible oxidation peaks at about  $E_{1/2} = 0.10$  and 0.80 V vs. NHE are assigned to the  $\text{Ru}^{\text{II,III}}/\text{Ru}^{\text{III,III}}$  and  $\text{Ru}^{\text{III,III}}/\text{Ru}^{\text{IV,IV}}$  redox couples, respectively. The third reversible peak that emerged at about  $E_{1/2} = 1.30$  V vs. NHE is assigned to the metal-based oxidation process of a  $\text{Ru}^{\text{IV,IV}}/\text{Ru}^{\text{V,V}}$  couple.

More electrochemical information could be obtained from the CV of complex **1** in a mixed  $\text{CF}_3\text{CH}_2\text{OH}/\text{pH}$  1.0 aqueous solution (Fig. 3b). Two reversible redox peaks of complex **1** at  $E_{1/2} = 0.48$  and 0.84 V vs. NHE are assigned respectively to two processes of the  $\text{Ru}^{\text{II}}/\text{Ru}^{\text{III}}-\text{OH}_2$  and  $\text{Ru}^{\text{III}}-\text{OH}_2/\text{Ru}^{\text{IV}}-\text{OH}$  couples. In addition, the onset potential of the catalytic water oxidation curve is found at 1.10 V vs. NHE. The redox processes observed at pH 1.0 conditions correspond to  $\text{Ru}^{\text{II}} \rightarrow \text{Ru}^{\text{III}}-\text{OH}_2 \rightarrow \text{Ru}^{\text{IV}}-\text{OH}$ . Owing that the  $\text{Ru}-\text{bda}$  complex carrying negatively charged ligands ( $\text{R}-\text{COO}^-$ ) possesses a low oxidation potential, high oxidation state intermediate  $\text{Ru}^{\text{V}}=\text{O}$  should be formed during the water oxidation process, but which would be difficult to observe because of the overlap of a catalytic water oxidation current. Meanwhile, it is also



Scheme 1. Synthetic route for the preparation of complex **1**.

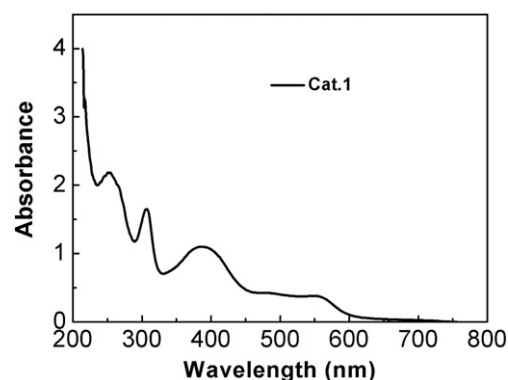


Fig. 2. Electronic absorption spectrum of complex **1** (1 mM) in  $\text{CH}_2\text{Cl}_2$ .

observed that complex **1** displays a low catalytic current compared to the reported  $\text{Ru}-\text{bda}$  type of catalysts.

The catalytic water oxidation activity of catalyst **1** was measured in a 100 mL round-bottomed flask, with  $(\text{NH}_4)_2[\text{Ce}^{\text{IV}}(\text{NO}_3)_6]$  (980 mg, 0.526 M) as oxidant and triflic acid (10%  $\text{CF}_3\text{CH}_2\text{OH}$ , 3.4 mL,  $\text{pH} = 1.0$ ) aqueous solution as solvent. The concentration of the catalyst is  $5.88 \times 10^{-5}$  M ( $[\text{catalyst}]/[\text{Ce}^{\text{IV}}] \approx 1/9000$ ). The generated oxygen was recorded with an oxygen sensor and calibrated by GC (Fig. 4). Based on the generated oxygen and the amount of catalyst molecules, the TON of catalyst **1** is calculated to be 900 (450 per ruthenium atom). By contrast, the dinuclear catalyst **1** shows a lower efficiency than the reported dinuclear ruthenium catalyst [17], even lower than the mononuclear catalyst with a similar catalytic center. The low efficiency of complex **1** obtained here is in agreement with its low electrochemical catalytic current. These results indicate that the steric effect of

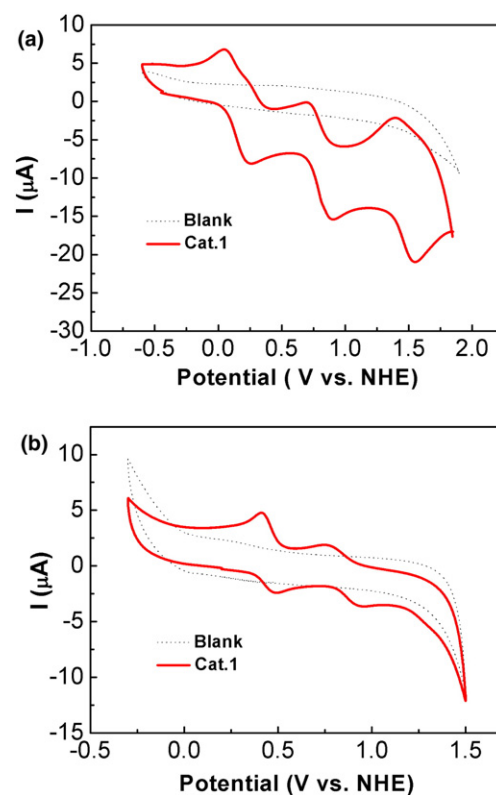


Fig. 3. (a) CV of complex **1** (1.0 mM) in  $\text{CH}_2\text{Cl}_2$ ; (b) CV of complex **1** (1.0 mM) in  $\text{HClO}_4$  aqueous solution (pH 1.0) containing 50%  $\text{CF}_3\text{CH}_2\text{OH}$ . A glassy carbon disk as the working electrode, a platinum wire as the counting electrode, and  $\text{Ag}/\text{AgNO}_3$  in  $\text{CH}_2\text{Cl}_2$  ( $\text{Ag}/\text{AgCl}$  in aqueous) as the reference electrode fitted to a one-compartment cell. Scan rate is  $100 \text{ mVs}^{-1}$ , calibration with the  $\text{Fc}/\text{Fc}^+$  is  $E_{1/2} = 0.56$  V vs. NHE, and  $\text{Ru}(\text{bpy})_3^{2+}/\text{Ru}(\text{bpy})_3^{3+}$  is  $E_{1/2} = 1.26$  V vs. NHE.

Download English Version:

<https://daneshyari.com/en/article/1305439>

Download Persian Version:

<https://daneshyari.com/article/1305439>

[Daneshyari.com](https://daneshyari.com)